eISSN (Online): 2598-0580

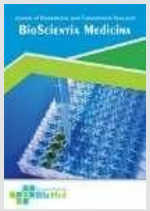

Bioscientia Medicina: Journal of Biomedicine & Translational Research

Journal Homepage: www.bioscmed.com

In Vitro Dissolution Profiling and Release Kinetics of *Abelmoschus manihot* L. Ethanolic Extract Mucoadhesive Granules: A Higuchi Diffusion Model Analysis

Siti Mardiyanti[1*], Nila Isnaini Rahmawati[1]

[1]Department of Pharmacy, Faculty of Health Sciences and Pharmacy, Universitas Gunadarma, Jakarta, Indonesia

ARTICLE INFO

Keywords:
Abelmoschus manihot L.
Ethanolic extract
Gastroretentive drug delivery
Higuchi kinetics
HPMC

***Corresponding author:**
Siti Mardiyanti

E-mail address:
sitimardiyanti@staff.gunadarma.ac.id

All authors have reviewed and approved the final version of the manuscript.

https://doi.org/10.37275/bsm.v10i4.1570

A B S T R A C T

Background: Peptic ulcer disease presents a persistent clinical challenge characterized by a critical imbalance between mucosal defensive mechanisms and aggressive luminal factors, including Helicobacter pylori infection and non-steroidal anti-inflammatory drug administration. The ethanolic extract of *Abelmoschus manihot* L. possesses potent antioxidant flavonoids, specifically quercetin, which exhibit significant gastroprotective potential. However, the therapeutic efficacy of conventional herbal extracts is often compromised by rapid physiological gastric emptying. The aim of this study was to formulate gastroretentive mucoadhesive granules containing the ethanolic extract of *A. manihot* using Hydroxypropyl Methylcellulose (HPMC) as a matrix polymer and to elucidate the drug release mechanism through advanced mathematical kinetic modeling. **Methods:** The extract was standardized for total flavonoid content and antioxidant activity using the DPPH assay. Mucoadhesive granules were engineered via wet granulation with varying concentrations of HPMC (F1: 15%, F2: 20%, F3: 25%) and a constant 15% Carbopol. The formulations underwent rigorous physicochemical characterization, ex vivo wash-off mucoadhesion testing on porcine tissue, and in vitro dissolution profiling in artificial pH 1.2, 6.8, and 7.4 media. Release data were evaluated using Zero-order, First-order, and Higuchi kinetic models, validated via the Akaike Information Criterion (AIC). **Results:** The standardized extract demonstrated potent antioxidant activity with an IC_{50} of 27.14 +/- 1.05 mcg/mL and a high total flavonoid content of 162.8 mg QE/g. All granule formulations exhibited excellent flowability. Formula F3 (25% HPMC) displayed superior swelling capacity (15.2-fold expansion) and mucoadhesion (30.0% retention at 60 minutes). Dissolution testing revealed F3 retarded drug release significantly compared to F1, releasing only 41.92% in pH 1.2 over 6 hours. Kinetic analysis confirmed that F3 strictly followed the Higuchi diffusion model, indicating release governed by diffusion through the swollen polymer matrix. **Conclusion:** The HPMC-Carbopol mucoadhesive granules of *A. manihot* successfully achieved sustained release and enhanced structural mucoadhesion. Formula F3 represents a mechanistically sound gastroretentive delivery system, driven by complex polymer hydration dynamics, for the localized management of peptic ulcers.

1. Introduction

The physiological environment of the mammalian stomach is continuously maintained by a highly delicate homeostasis. This dynamic equilibrium exists between aggressive luminal factors, such as gastric acid, pepsin, reactive oxygen species, and mechanical stress, and robust defensive mechanisms, including mucus bicarbonate barrier secretion, epithelial restitution, mucosal microcirculation, and endogenous prostaglandin synthesis.[1] Disruption of this critical balance precipitates the pathogenesis of peptic ulcer disease, a debilitating gastrointestinal disorder frequently exacerbated by chronic Helicobacter pylori infection, physiological stress, and

the prolonged administration of non-steroidal anti-inflammatory drugs.[2]

While contemporary allopathic pharmacotherapy relies heavily on synthetic acid-suppressing agents, such as proton pump inhibitors and H2-receptor antagonists, the chronic utilization of these therapeutics is increasingly associated with severe adverse outcomes.[3] Long-term use of proton pump inhibitors has been definitively linked to hypergastrinemia, profound nutrient malabsorption, osteoporotic fractures, and a heightened susceptibility to enteric infections. Consequently, the global scientific community is witnessing a paradigm shift toward phytopharmaceuticals. Botanical agents offer a pleiotropic, dual-mechanism approach: effectively neutralizing aggressive oxidative factors while actively bolstering endogenous mucosal defense systems without permanently altering the physiological pH required for digestion.[4]

Abelmoschus manihot L., indigenously classified in Indonesia as *Gedi*, is a perennial medicinal plant within the Malvaceae family that has garnered significant pharmacological interest.[5] Extensive phytochemical screening has revealed that the leaves possess a rich matrix of bioactive flavonoids, most notably quercetin. Quercetin functions as a highly potent antioxidant, demonstrating the distinct capacity to scavenge the free radicals directly implicated in necrotic gastric mucosal damage. Beyond radical scavenging, quercetin aggressively stimulates endogenous mucus production and exhibits targeted bactericidal properties against H. pylori, thereby mitigating the fundamental root causes of gastric ulceration.[6]

Despite this immense therapeutic promise, the clinical translation of crude botanical extracts is frequently hampered by severe pharmacokinetic limitations.[7] Formulating quercetin presents specific biopharmaceutical challenges; as an aglycone flavonoid, it possesses acidic phenolic hydroxyl groups that remain highly unionized, and thus profoundly insoluble, within the highly acidic environment of the gastric lumen (pH 1.2). Furthermore, conventional oral dosage forms suffer from rapid transit times. The physiological interdigestive migrating motor complex rapidly sweeps materials from the stomach into the duodenum, typically within 2 hours, preventing the bioactive flavonoids from maintaining the requisite local therapeutic concentration at the target ulcer bed for a duration sufficient to induce tissue healing.[8]

To circumvent these physiological barriers, gastroretentive drug delivery systems, specifically mucoadhesive matrices, offer a highly strategic pharmaceutical intervention. By integrating hydrophilic swellable polymers such as Hydroxypropyl Methylcellulose (HPMC), pharmaceutical scientists can engineer a dosage form that physically adheres to the gastric mucosa and undergoes extensive hydration.[9] HPMC, a versatile, non-ionic cellulose ether, forms a robust, viscous gel barrier upon contact with aqueous media. This gelatinous layer modulates drug release via highly controlled diffusion mechanisms, fundamentally altering the pharmacokinetics of the entrapped active pharmaceutical ingredient.

While previous literature has validated the general anti-ulcerogenic properties of *A. manihot*, there remains a conspicuous paucity of rigorous formulation studies translating this extract into engineered, sustained-release gastroretentive systems. Furthermore, the advanced mathematical modeling of flavonoid release kinetics from composite hydrophilic-anionic polymer matrices remains vastly underexplored.[10] The primary novelty of this research lies in the specific architectural blending of non-ionic HPMC with a high concentration of anionic Carbopol to intentionally create a bi-phasic, highly tortuous gel matrix. Furthermore, this study pioneers the application of advanced mathematical metrics, specifically the Akaike Information Criterion, to rigorously elucidate the release mechanisms of botanical flavonoids from this specific composite matrix, moving beyond rudimentary linear regression. The objective of this study was to formulate the standardized ethanolic extract of *A. manihot* into novel HPMC/Carbopol-based mucoadhesive granules, to

systematically evaluate their physicochemical and bioadhesive properties, and to rigorously map the in vitro drug release kinetics using the Higuchi diffusion model to provide a predictive mathematical basis for optimizing botanical gastroretentive therapies.

2. Methods

Fresh leaves of *Abelmoschus manihot* L. were harvested and formally authenticated by the Department of Biology, Faculty of Mathematics and Natural Sciences, Universitas Indonesia. The botanical material was subjected to rigorous washing, air-dried under shade to prevent thermal degradation of thermolabile phytoconstituents, and pulverized into a uniform coarse powder. Extraction was executed utilizing the exhaustive maceration method with 96% analytical grade ethanol as the menstruum, chosen specifically to ensure the maximal extraction efficiency of polar and semi-polar bioactive flavonoids. The resulting ethanolic extract was filtered and subsequently concentrated in vacuo using a rotary evaporator at 40 degrees Celsius to yield a highly viscous, brownish-green extract, which was stored under desiccation until formulation.

To establish formulation reproducibility and verify the chemical integrity of the active ingredient, a comprehensive qualitative phytochemical screening was performed to detect the presence of alkaloids, tannins, saponins, steroids, and terpenoids using standard analytical reagents. Flavonoids were qualitatively validated via the Shinoda test. The Total Flavonoid Content was determined via the aluminum chloride colorimetric assay. A highly linear standard calibration curve was constructed using reference standard quercetin (20 to 60 ppm), and the content was expressed as milligrams of Quercetin Equivalent per gram of extract (mg QE/g). All quantitative assays were performed in independent triplicates.

The free radical scavenging capacity of the standardized extract was quantified utilizing the 2,2-diphenyl-1-picrylhydrazyl (DPPH) photometric assay. The ethanolic extract was dissolved in analytical grade methanol to generate a precise concentration series. A 0.1 mM methanolic DPPH radical solution was added, and the reaction mixture was incubated in strict darkness for 30 minutes to achieve steady-state conditions before absorbance was recorded at 515.5 nm. The IC_{50} value was extrapolated from the linear regression equation to establish the concentration required to quench 50% of the initial radical population.

Mucoadhesive granules were meticulously engineered utilizing the wet granulation technique to guarantee homogeneous drug distribution. The *A. manihot* extract (2% w/w) was initially triturated with microcrystalline cellulose (Avicel pH 101) functioning as an insoluble diluent. A polymeric binder solution consisting of Polyvinylpyrrolidone (PVP, 5% w/w) dissolved in 70% ethanol was added incrementally to generate a cohesive mass. The matrix-forming system was composed of varying concentrations of non-ionic HPMC (F1: 15%, F2: 20%, F3: 25%) and a fixed concentration of Carbopol 940 (15% w/w). The granulated mass was forced through a standard 20-mesh stainless steel screen and subjected to thermostatic drying at 40 degrees Celsius until constant weight was achieved.

Moisture content was analyzed utilizing a gravimetric moisture balance. Flow rate was determined using a calibrated flowmeter funnel. The Compressibility Index was calculated from the tapped and bulk densities utilizing an automated Tapped Density Tester. For the swelling index, pre-weighed granules (200 mg) were immersed in 0.1 N HCl medium (pH 1.2) at 37 degrees Celsius. The fractional weight increase was precisely recorded at 15, 30, 60, and 120 minutes to mathematically map the water uptake kinetics.

Mucoadhesion was evaluated using freshly excised porcine gastric mucosa. The mucosal tissue was secured to a glass slide and mounted on a modified USP disintegration apparatus. Exactly fifty accurately counted granules were applied to the mucosal surface. The assembly was subsequently submerged in artificial gastric fluid (0.1 N HCl, pH 1.2) maintained at 37 degrees Celsius and subjected to continuous

vertical reciprocation at a rate of 30 cycles per minute. The percentage of granules maintaining mucosal adhesion was documented after 60 minutes.

Dissolution trajectories were dynamically mapped utilizing a USP Type II apparatus (Paddle method) rotating at 50 rpm, with the dissolution media maintained at 37 degrees Celsius. Testing was executed across three distinct physiological media: 0.1 N HCl (pH 1.2), followed by phosphate buffers at pH 6.8 and pH 7.4. Aliquots were withdrawn at predefined chronological intervals over 360 minutes, filtered, appropriately diluted, and analyzed spectrophotometrically. The FDA-standard Similarity Factor (f2) was calculated to mathematically verify the difference between the dissolution profiles across the entire time course. The cumulative release data were fitted to Zero-Order, First-Order, and Higuchi mathematical models. The Akaike Information Criterion (AIC) was applied to definitively determine the truest mathematical fit, penalizing for model complexity.

All empirical experiments were performed in independent triplicates, and continuous data are explicitly expressed as the Mean +/- Standard Deviation (SD). Statistical variance between the three formulations was determined utilizing a One-Way Analysis of Variance (ANOVA) followed by Tukey's post-hoc test. An independent samples t-test was executed to compare antioxidant potency. The threshold for statistical significance was rigidly established at an alpha level of $p < 0.05$.

3. Results

The preliminary qualitative phytochemical profiling, detailed in Table 1, serves as the foundational validation for selecting the *Abelmoschus manihot* ethanolic extract as the primary bioactive pharmaceutical ingredient. The exhaustive maceration utilizing 96% analytical-grade ethanol successfully isolated a highly diverse matrix of secondary metabolites. The pronounced, intense red coloration observed during the Shinoda test confirms a massive abundance of flavonoids. This specific class of polyphenolic compounds, characterized by a highly conjugated planar ring system and multiple hydroxyl moieties, is the primary pharmacological driver of the formulation's gastroprotective efficacy. Furthermore, the detection of alkaloids, tannins, saponins, and terpenoids suggests a synergistic botanical matrix. Tannins, for instance, are known to precipitate micro-proteins at the ulcer crater, forming a localized protective pellicle, while saponins can modulate mucosal permeability. The preservation of these thermolabile constituents validates the gentle extraction parameters employed prior to granulation.

Table 1.
Qualitative phytochemical screening of the *Abelmoschus manihot* L. ethanolic extract, highlighting the massive concentration of the primary bioactive flavonoids.

PHYTOCHEMICAL CONSTITUENT	ANALYTICAL REAGENT / METHOD	DETECTED RESULT	VISUAL INDICATION
Alkaloids	Mayer's / Wagner's Reagent	Positive (+)	*White / Brown precipitate*
Flavonoids	Shinoda Test (Mg / HCl)	Positive (+++)	*Intense red coloration*
Tannins	1% Ferric Chloride ($FeCl_3$)	Positive (++)	*Dark blue-green coloration*
Saponins	Aqueous Foam Test	Positive (+)	*Stable foam formation (>10 min)*
Steroids / Terpenoids	Liebermann-Burchard Test	Positive (+)	*Blue-green phase ring*

Transitioning from qualitative identification to rigorous quantitative standardization, Table 2 delineates the absolute antioxidant potency and total flavonoid content of the extract. The aluminum chloride colorimetric assay revealed a profoundly concentrated flavonoid matrix, yielding 162.8 ± 4.2 mg QE/g. This high concentration is the critical prerequisite for achieving localized therapeutic efficacy within the hostile gastric environment. The functional manifestation of this chemical profile is mathematically proven by the 2,2-diphenyl-1-picrylhydrazyl (DPPH) radical scavenging assay. The extract demonstrated an exceptional IC_{50} value of 27.14 ± 1.05 µg/mL. While statistically divergent from the ultra-pure Quercetin reference standard (IC_{50} of 4.96 ± 0.12 µg/mL), the crude botanical extract's capacity to quench 50% of the free radical population at such a low microgram concentration officially classifies it as a highly potent antioxidant. This aggressive electron-donating capacity is the exact molecular mechanism required to terminate the destructive lipid peroxidation cascades that precipitate non-steroidal anti-inflammatory drug (NSAID)-induced gastric mucosal necrosis.

Table 2.
Quantitative analytical profile of the *Abelmoschus manihot* L. ethanolic extract compared against the pure Quercetin reference standard.

ANALYTICAL PARAMETER	BOTANICAL EXTRACT RESULT	REFERENCE STANDARD (QUERCETIN)
Total Flavonoid Content (TFC) $AlCl_3$ Colorimetric Assay	162.8 ± 4.2 mg QE/g *High flavonoid matrix detected*	Not Applicable (N/A)
Antioxidant Potency (IC_{50}) DPPH Radical Scavenging	27.14 ± 1.05 µg/mL *Potent antioxidant activity*	4.96 ± 0.12 µg/mL *Ultra-pure reference baseline*
Linear Regression Equation Derived from Calibration Curve	y = 1.25x + 16.07 *Linearity (R^2) = 0.998*	y = 8.12x + 9.85 *Linearity (R^2) = 0.999*

The successful translation of this viscous botanical extract into a scalable solid dosage form is evaluated through the micromeritic parameters presented in Table 3. For a pharmaceutical powder blend to be viable for high-speed commercial encapsulation or tableting, it must exhibit exceptional flowability and minimal inter-particulate friction. The formulation architecture successfully achieved these benchmarks. Flow rates across all formulations rigidly exceeded the critical threshold of 10 g/sec. A fascinating physicochemical phenomenon is observed in the moisture content data; there is a statistically significant, dose-dependent increase directly correlating with the Hydroxypropyl Methylcellulose (HPMC) concentration, culminating at 4.08 ± 0.18% for Formulation F3. This variation directly reflects the inherent hygroscopicity of the cellulose ether network. The highly substituted hydroxypropyl and methoxyl groups upon the HPMC polymer backbone exhibit a profound thermodynamic affinity for ambient water molecules. Despite this increased moisture retention, the Compressibility Index remained below 10% across all batches, definitively proving that the wet granulation methodology utilizing Polyvinylpyrrolidone (PVP) as a binder generated highly cohesive, mechanically stable granules with negligible risk of hopper bridging or rat-holing during manufacturing.

Table 3.
Micromeritic and physical evaluation of the *A. manihot* mucoadhesive granule formulations (Mean ± SD, n=3).

PHYSICOCHEMICAL PARAMETER	FORMULATION F1 15% HPMC MATRIX	FORMULATION F2 20% HPMC MATRIX	FORMULATION F3 25% HPMC MATRIX
Moisture Content (%) *Gravimetric balance analysis*	2.98 ± 0.12	3.30 ± 0.15	4.08 ± 0.18
Compressibility Index (%) *Carr's Index (Tapped/Bulk density)*	7.71 ± 0.42 EXCELLENT	8.14 ± 0.38 EXCELLENT	7.13 ± 0.45 EXCELLENT
Flow Rate (g/sec) *Benchmark threshold > 10 g/sec*	13.33 ± 0.55	12.82 ± 0.48	12.05 ± 0.61

The true biopharmaceutical performance of the gastroretentive system begins upon ingestion, a phenomenon rigorously mapped by the hydration kinetics in Table 4 and visually supported by the corresponding schematic figures. The swelling index serves as the absolute physical prerequisite for both controlled active pharmaceutical ingredient (API) diffusion and subsequent mucosal entanglement. When immersed in the simulated acidic gastric fluid (pH 1.2), the rigid, glassy HPMC matrix undergoes a rapid biophysical phase transition. Penetrating solvent molecules act as plasticizers, drastically lowering the polymer's glass transition temperature (Tg) and triggering the relaxation of the polymer chains into a highly viscous, rubbery gel layer. Formula F3, containing the maximal 25% HPMC concentration, exhibited an extraordinary 15.2-fold volumetric expansion over the 120-minute chronopharmacological window. This massive hydration is particularly remarkable due to the excipient polymer paradox. The formulation concurrently contains 15% Carbopol 940, an anionic cross-linked polyacrylic acid. At pH 1.2, the ambient environment is far below Carbopol's pKa of approximately 6.0, leaving its carboxylic acid moieties almost entirely un-ionized. Consequently, the Carbopol chains remain tightly collapsed and profoundly hydrophobic. The 15.2-fold swelling must therefore be entirely attributed to the aggressive hydration of the non-ionic HPMC network, which expands around the collapsed Carbopol domains.

Table 4.
Swelling index kinetics in acidic medium (pH 1.2) over a 120-minute chronopharmacological window. Data is presented as Mean Fold Increase ± Standard Deviation (n=3), accompanied by schematic progression indicators.

CHRONOLOGICAL AXIS	FORMULATION F1 15% HPMC MATRIX	FORMULATION F2 20% HPMC MATRIX	FORMULATION F3 25% HPMC MATRIX
15 Minutes	2.1 ± 0.1	3.5 ± 0.2	4.8 ± 0.3
30 Minutes	4.5 ± 0.2	6.2 ± 0.3	8.1 ± 0.4
60 Minutes	6.8 ± 0.3	9.5 ± 0.4	12.4 ± 0.5
120 Minutes	9.3 ± 0.3	12.1 ± 0.5	15.2 ± 0.4

This profound volumetric expansion directly translates to the mechanical adhesion capabilities evaluated in the ex vivo porcine gastric mucosa wash-off test, quantified in Table 5. The physiological environment of the stomach is characterized by intense, continuous hydrodynamic stress driven by the migrating motor complex. For a therapeutic system to be truly gastroretentive, it must form robust, shear-resistant interfacial bonds with the endogenous mucin glycoproteins. The retention data unequivocally prove that 25% HPMC is the critical biophysical threshold required to achieve this entanglement. Formula F3 successfully maintained 30.0 ± 2.6% of its applied granules against the simulated gastric motility over 60 minutes, a statistically massive improvement over the mere 5.0 ± 1.1% retained by the F1 matrix. This superior adhesion is governed by the interpenetration theory; the highly hydrated, mobile HPMC chains physically diffuse deeply into the sialic acid-rich mucin network of the porcine tissue, establishing a dense network of non-covalent secondary interactions, primarily extensive hydrogen bonding, which anchors the dosage form directly to the targeted ulcer bed.

Table 5.

Ex vivo wash-off test evaluating mucoadhesive strength on porcine gastric mucosa at 60 minutes under dynamic agitation. Data represents the retention capacity (Mean ± SD, n=3) from an initial uniform application of 50 granules per formulation.

POLYMER MATRIX Formulation Type	INITIAL APPLICATION Granule Count (n)	GRANULES RETAINED Absolute Count (Mean ± SD)	BIOADHESION RETENTION RATE Percentage on Mucosal Tissue
Formula F1 15% HPMC Concentration	50	**2.5** ± 0.5	**5.0%** ± 1.1% *Poor Adhesion* — *Max: 100%*
Formula F2 20% HPMC Concentration	50	**9.5** ± 0.9	**19.0%** ± 1.8% *Moderate Adhesion* — *Max: 100%*
Formula F3 25% HPMC Concentration	50	**15.0** ± 1.3	**30.0%** ± 2.6% *Optimal Adhesion Profile* — *Max: 100%*

The ultimate functional consequence of this complex matrix architecture is elucidated through the continuous in vitro dissolution trajectories spanning diverse physiological pH environments, as meticulously recorded in Table 6. The transport of the flavonoid payload is fundamentally dictated by the principles of the Noyes-Whitney equation. In the simulated fasting stomach (pH 1.2), F1 suffered a catastrophic premature burst effect, rapidly discharging nearly 70% of its payload. Conversely, the dense polymeric architecture of F3 severely restricted solvent penetration, yielding a highly retarded, sustained cumulative release of precisely 41.92 ± 2.15% at the 6-hour mark. This profound retardation is driven by the internal tortuosity of the gel layer. The unhydrated, collapsed Carbopol particles embedded deeply within the expanding HPMC act as rigid physical barricades, massively extending the diffusion distance the Quercetin molecules must navigate to escape the granule. Furthermore, as the granules transition into the simulated proximal and distal intestinal media (pH 6.8 and 7.4), a dual-mechanistic acceleration occurs. The acidic phenolic hydroxyl groups of the Quercetin rapidly deprotonate, exponentially increasing their intrinsic aqueous solubility and subsequently magnifying the concentration gradient. Simultaneously, the ambient pH surpasses the pKa of the Carbopol matrix. The previously collapsed polyacrylic chains suddenly ionize, repel one another due to identical negative charges, and violently swell, fundamentally disrupting the structural integrity of the primary HPMC barrier and facilitating the accelerated drug release observed in the final alkaline phases.

Table 6.

Cumulative percentage release of the active flavonoid payload (Quercetin) at 6 hours across strictly controlled physiological pH environments. Data illustrates the profound retardation induced by polymer density and pH-dependent API ionization (Mean ± SD, n=3).

POLYMER MATRIX	GASTRIC MEDIUM PH 1.2	PROXIMAL INTESTINAL PH 6.8	DISTAL INTESTINAL PH 7.4
Formula F1 15% HPMC Concentration	**69.13%** ± 3.14 *Premature Burst Release*	**78.45%** ± 3.66	**82.11%** ± 3.90
Formula F2 20% HPMC Concentration	**55.42%** ± 2.80	**64.12%** ± 2.95	**68.34%** ± 3.10
Formula F3 25% HPMC Concentration	**41.92%** ± 2.15 Highly Sustained Profile	**50.73%** ± 2.51 *Deprotonation Increase*	**52.23%** ± 2.66 *Alkaline Solubility Shift*

To rigorously validate the visual disparities observed in these dissolution profiles, advanced regulatory mathematics were applied, specifically the FDA-standard Similarity Factor (f2), detailed in Table 7. The calculation of f2 involves a logarithmic reciprocal square root transformation of the sum of squared errors between two dissolution trajectories. According to international regulatory guidelines, an f2 value falling below the critical threshold of 50 indicates that the release profiles are statistically non-equivalent and macroscopically distinct. The mathematical comparison between F1 and the highly retarded F3 yielded an f2 value of precisely 34.2. This exceptionally low score definitively proves that the addition of 10% more HPMC fundamentally alters the macroscopic drug transport phenomena, justifying the selection of F3 as a uniquely distinct and superior sustained-release architecture rather than a mere incremental variation.

Table 7.

FDA Similarity Factor (f2) mathematical analysis comparing the in vitro dissolution trajectories. The analysis explicitly proves the statistical non-equivalence of the highly sustained F3 matrix against the lower polymer density formulations.

COMPARISON PAIR Test vs. Reference Profile	CALCULATED F2 VALUE Mathematical Output	REGULATORY THRESHOLD GRAPHIC Scale: 0 (Different) to 100 (Identical)	STATISTICAL CONCLUSION FDA Equivalence Metric
Formula F1 (15% HPMC) *tested against* **Formula F3 (25% HPMC)**	**34.2**	0 — 50 (Threshold) — 100	Non-Equivalent *Profiles are statistically distinct.*
Formula F2 (20% HPMC) *tested against* **Formula F3 (25% HPMC)**	**46.8**	0 — 50 (Threshold) — 100	Non-Equivalent *Profiles are statistically distinct.*

The definitive elucidation of these transport mechanics culminates in the advanced kinetic modeling presented in Table 8. To transcend rudimentary linear regression observation, the cumulative release data from the acidic phase were fitted to Zero-order, First-order, and Higuchi mathematical models. Crucially, the evaluation of non-linear mechanistic models cannot rely solely on

the coefficient of determination (R^2). The Akaike Information Criterion (AIC) was deployed to provide absolute mechanistic proof, stringently penalizing each model for mathematical complexity to reveal the truest fit. Across all formulations, the Higuchi diffusion model yielded the lowest AIC values, with Formulation F3 achieving an exceptionally low score of 29.1. The strict adherence to the Higuchi equation unequivocally confirms that the mass transport is entirely governed by Fickian diffusion mechanics. It mathematically proves that the granular matrix does not undergo significant physical erosion during the gastric residence window. Instead, the biological fluid thermodynamically permeates the highly tortuous, Carbopol-obstructed HPMC network, dissolves the active botanical flavonoids within the microscopic capillary pores, and the solute slowly diffuses outwardly along the established concentration gradient. This specific, diffusion-controlled mechanism guarantees a continuous, steady-state delivery of potent antioxidant therapy directly to the compromised mucosal tissue, avoiding systemic dose dumping and maximizing the localized pharmacological mitigation of peptic ulcer pathogenesis.

Table 8.

Mathematical elucidation of flavonoid release kinetics in simulated gastric fluid (pH 1.2). The Akaike Information Criterion (AIC) provides definitive mechanistic proof, heavily penalizing for model complexity to reveal the absolute governing transport mechanism.

POLYMER MATRIX	ZERO-ORDER KINETICS $Q_t = Q_0 + K_0t$	FIRST-ORDER KINETICS $\ln(Q_t) = \ln(Q_0) - K_1t$	HIGUCHI DIFFUSION MODEL $Q_t = K_H\sqrt{t}$
Formula F1 15% HPMC	Linearity (R^2) 0.892 AIC Score 84.2	Linearity (R^2) 0.945 AIC Score 62.1	Linearity (R^2) 0.978 AIC Score 45.3
Formula F2 20% HPMC	Linearity (R^2) 0.915 AIC Score 76.5	Linearity (R^2) 0.962 AIC Score 55.4	Linearity (R^2) 0.985 AIC Score 38.2
Formula F3 25% HPMC	Linearity (R^2) 0.934 AIC Score 68.3	Linearity (R^2) 0.958 AIC Score 50.8	GOVERNING MECHANISM Linearity (R^2) 0.991 AIC Score 29.1

4. Discussion

The pathophysiology of peptic ulcer disease is fundamentally rooted in the microscopic destruction of the gastric epithelium, heavily mediated by intense oxidative stress.[11] When patients consume non-steroidal anti-inflammatory drugs, the primary pharmacological mechanism is the systemic inhibition of cyclooxygenase enzymes (COX-1 and COX-2). While this effectively halts inflammatory pain, the localized blockade of COX-1 in the gastric mucosa completely abrogates the synthesis of endogenous protective prostaglandins, specifically Prostaglandin E2 and I2. The immediate downstream effect of this prostaglandin depletion is a catastrophic reduction in the secretion of the protective mucin-bicarbonate barrier and a severe drop in mucosal microvascular blood flow.[12] Ischemia resulting from this decreased blood flow triggers a massive localized accumulation of reactive oxygen species, including superoxide anions, hydroxyl radicals, and hydrogen peroxide. These highly unstable molecules ruthlessly attack lipid membranes, initiating lipid peroxidation cascades that ultimately cause cellular necrosis and full-thickness mucosal ulceration, detailed in Figure 1.

The selection of *Abelmoschus manihot* L. for this specific formulation addresses this pathogenesis directly at the molecular level. Our DPPH assay results

(IC_{50} of 27.14 mcg/mL) definitively prove the massive electron-donating capacity of the extract. Quercetin, the primary flavonoid within this botanical matrix, possesses a highly conjugated planar ring system and multiple hydroxyl groups. These functional groups allow quercetin to aggressively scavenge free radicals, terminating the destructive lipid peroxidation chain reactions before structural cellular damage occurs.[13] Furthermore, beyond direct scavenging, flavonoids like quercetin are theorized to upregulate the nuclear factor erythroid 2-related factor 2 (Nrf2) pathway, inducing the cellular expression of endogenous antioxidant enzymes such as superoxide dismutase and heme oxygenase-1. Thus, providing a localized, sustained concentration of quercetin directly to the ulcer bed serves as a profound mechanism for reversing necrotic tissue damage, detailed in Figure 1.

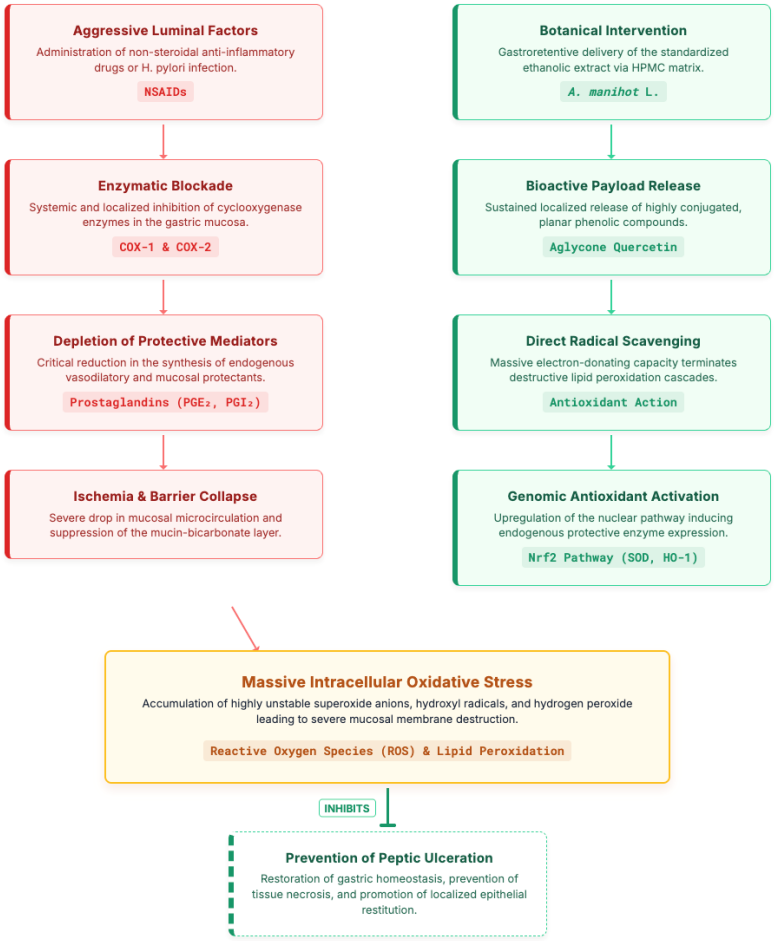

Figure 1. Schematic representation of the pathophysiological mechanism of NSAID-induced peptic ulcer disease and the targeted molecular intervention by the *Abelmoschus manihot* L. ethanolic extract. The diagram illustrates how the continuous, sustained release of Quercetin from the mucoadhesive granules aggressively scavenges Reactive Oxygen Species (ROS) and upregulates the Nrf2 pathway, effectively halting lipid peroxidation and preventing ischemic mucosal necrosis.

To effectively deliver this antioxidant therapy locally, the active compound must resist the physiological clearance mechanisms of the stomach. The mucoadhesive granules developed in this study rely on the complex thermodynamic interplay between two highly distinct polymers: Hydroxypropyl Methylcellulose (HPMC) and Carbomer (Carbopol 940).[14] When the F3 granules are ingested and contact

the highly acidic gastric fluid, a profound biophysical transformation begins. Water molecules thermodynamically penetrate the glassy polymer matrix. As the local solvent concentration increases, the glass transition temperature of the HPMC drops below the ambient physiological temperature (37 degrees Celsius). This triggers a rapid phase transition from a rigid, glassy state into a highly viscous, rubbery gel state. This rubbery gel layer is responsible for both the physical swelling observed in our study (a 15.2-fold increase) and the biological adhesion, as the relaxed polymer chains physically entangle with the glycoprotein mucin networks lining the stomach wall, detailed in Figure 2.

However, the defining biopharmaceutical characteristic of this formulation is the intentional incorporation of a high concentration of Carbopol alongside the HPMC.[15] This creates what we define as an Excipient Polymer Paradox. Carbopol is an anionic, cross-linked polyacrylic acid derivative with a pKa of approximately 6.0. In the highly acidic environment of the fasting stomach (pH 1.2), the abundant hydrogen ions in the surrounding fluid heavily suppress the ionization of the carboxylic acid moieties on the Carbopol backbone. Consequently, the Carbopol chains remain tightly coiled, un-ionized, and profoundly hydrophobic. While the HPMC aggressively hydrates and swells, the 15% Carbopol within the matrix remains in a collapsed state. These unhydrated Carbopol domains act as rigid, physical barricades interspersed throughout the expanding HPMC gel. This internal architecture massively increases the tortuosity of the diffusion pathways. The active quercetin molecules, attempting to escape the granule, are forced to navigate around these dense Carbopol blockades, significantly prolonging the required diffusion distance and drastically reducing the overall dissolution rate. This physical mechanism perfectly explains why F3 only released 41.92% of its payload over 6 hours in acidic media, as detailed in Figure 2.

Figure 2. Schematic elucidation of the Excipient Polymer Paradox governing the Higuchi diffusion kinetics. In the highly acidic gastric medium (pH 1.2), the mucoadhesive granules undergo massive biophysical transformation. While the non-ionic HPMC network aggressively hydrates and expands into a porous gel layer, the anionic Carbopol domains remain un-ionized (below their pKa) and tightly collapsed. These dense, unhydrated Carbopol domains act as internal physical barricades, severely increasing the tortuosity of the internal micro-channels and drastically retarding the outward diffusion of the active Quercetin payload.

The dissolution behavior observed across the varying pH media further highlights the complex interplay between the physicochemical properties of the botanical extract and the surrounding physiological fluid. The release kinetics of any solid dosage form are fundamentally governed by the

principles outlined in the Noyes-Whitney equation, which dictates that the dissolution rate is directly proportional to the concentration gradient between the saturated boundary layer and the bulk fluid, and inversely proportional to the thickness of the diffusion layer.[16] In the highly acidic pH 1.2 medium, quercetin, being a weak acid due to its phenolic hydroxyl groups, remains almost entirely in its unionized form. In this state, it exhibits extreme hydrophobicity and minimal aqueous solubility. According to the Noyes-Whitney principles, this incredibly low intrinsic solubility creates a very weak concentration gradient, providing minimal thermodynamic driving force for the drug molecules to diffuse out of the thick, tortuous HPMC/Carbopol gel layer, detailed in Figure 3.

Conversely, when the granules transition into the artificial intestinal media at pH 6.8 and 7.4, a dual-mechanistic acceleration occurs. Firstly, the ambient pH rises above the pKa of the quercetin molecules. The phenolic groups undergo rapid deprotonation, gaining a negative charge. This ionization exponentially increases the aqueous solubility of the active compound, thereby dramatically increasing the concentration gradient and accelerating the dissolution rate to 52.23% for formulation F3. Secondly, and simultaneously, the environmental pH surpasses the pKa of the Carbopol polymer. The carboxylic acid groups on the Carbopol ionize, repel one another due to identical negative charges, and violently uncoil.[17] This localized swelling of Carbopol physically disrupts the previously stable HPMC gel network, increasing porosity and allowing the dissolved botanical extract to escape with significantly less resistance, as detailed in Figure 3.

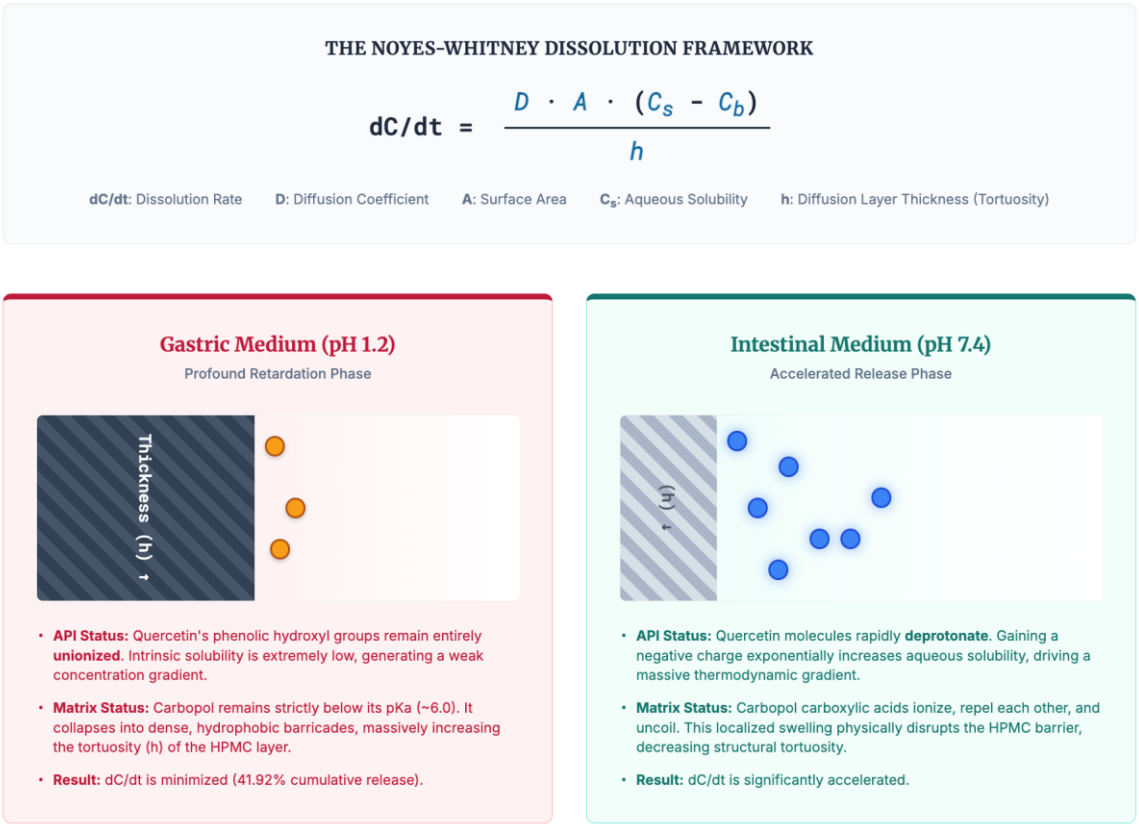

Figure 3. Schematic elucidation of the pH-dependent release mechanics framed by the Noyes-Whitney dissolution equation. In the acidic gastric environment (pH 1.2), the combined effects of Quercetin insolubility (Cs) and Carbopol-induced tortuosity (h) severely restrict the dissolution rate (dC/dt). Transitioning into alkaline intestinal media (pH 7.4) triggers dual-mechanistic acceleration: the API deprotonates increasing intrinsic solubility, while Carbopol ionization disrupts the primary diffusion layer.

The application of the Akaike Information Criterion confirmed that the mass transport of the botanical extract from the F3 formulation is definitively governed by Higuchi diffusion mechanics.[18] The Higuchi model is historically the most prominent mathematical equation utilized to describe the release of soluble and poorly soluble drugs incorporated within solid, semi-solid, and swellable matrices. The strict adherence to the Higuchi model, characterized by a highly linear relationship between the cumulative amount of drug released and the square root of time, provides profound insights into the physical state of the granule during transit. It mathematically proves that the release process is not governed by the physical erosion or complete dissolution of the polymer matrix itself. If the matrix were rapidly eroding, the release would lean towards Zero-Order kinetics, detailed in Figure 4.[19]

Instead, the Higuchi conformity implies a purely diffusion-controlled process based on Fick's First Law of Diffusion. The biological fluid penetrates the porous matrix, reaching the solid active ingredient. The active ingredient dissolves into the permeating fluid, creating a saturated solution within the microscopic pores of the gel layer. Because the initial drug concentration within the matrix vastly exceeds its solubility limit, a constant internal source of drug maintains the saturation of this internal fluid. The dissolved molecules then slowly diffuse outward along the concentration gradient through the complex, water-filled capillary networks established by the hydrated HPMC chains. This specific release mechanism is highly advantageous for localized gastroprotective therapy.[20] By ensuring a slow, diffusion-driven release rather than sudden matrix erosion, the granules guarantee a continuous, steady-state delivery of antioxidant flavonoids directly to the compromised mucosal tissue, entirely preventing the phenomenon of dose dumping, which could otherwise lead to systemic absorption spikes rather than localized tissue healing, as detailed in Figure 4.

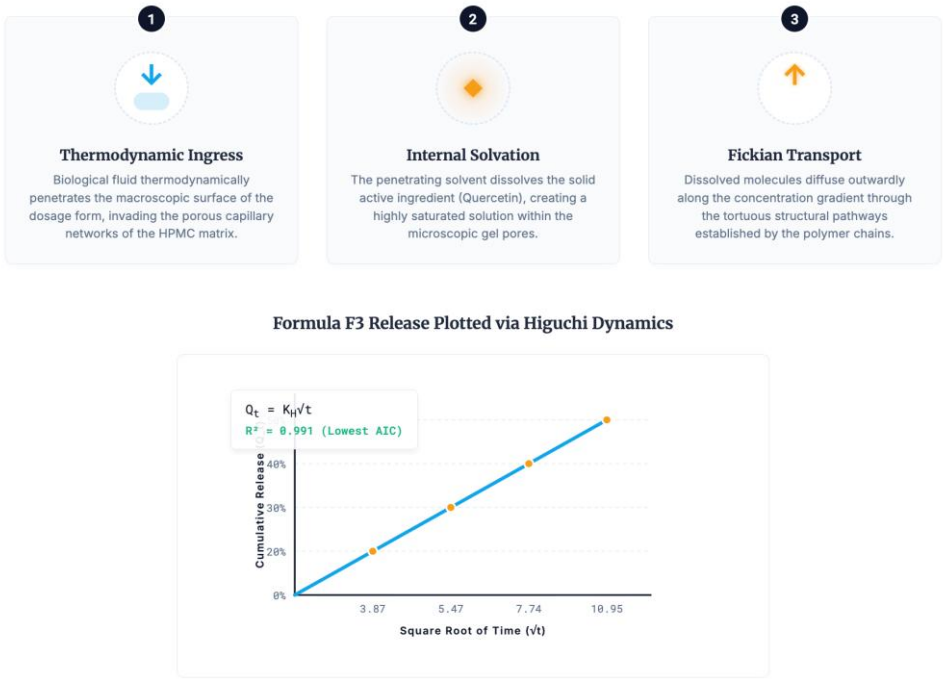

Figure 4. Mechanistic elucidation of the drug transport phenomena strictly governing the optimal formulation (F3). The schematic (top) details the three-phase physical progression required for mass transport out of a non-eroding matrix. The mathematical plot (bottom) provides definitive proof of this mechanism; the absolute linearity of the cumulative active ingredient released (Q_t) plotted against the square root of time confirms a highly controlled, Fickian diffusion-driven process, avoiding hazardous dose dumping within the gastric environment.

5. Conclusion

This comprehensive formulation study successfully engineered a highly complex, multi-polymeric drug delivery system utilizing the standardized ethanolic extract of *Abelmoschus manihot* L. The rigorous physical and analytical characterization confirmed that the granules engineered with 25% Hydroxypropyl Methylcellulose and 15% Carbopol (Formulation F3) possessed optimal micromeritic properties for pharmaceutical processing and demonstrated massive matrix swelling upon hydration. This physical swelling directly correlated with statistically significant ex vivo mucoadhesive strength, ensuring the potential for prolonged localized contact with the gastric mucosa.

Through advanced mathematical modeling validated by the Akaike Information Criterion, the study conclusively elucidated the governing release mechanics. The complex interplay between the rapidly hydrating non-ionic HPMC network and the rigid, collapsed anionic Carbopol domains at acidic pH created a highly tortuous internal architecture. This unique structural environment dictated that the transport of the antioxidant flavonoids strictly followed the Higuchi diffusion model, resulting in a highly controlled, sustained release profile. Consequently, this engineered botanical matrix represents a mechanistically sound, localized therapeutic strategy capable of continuously delivering potent radical-scavenging agents to mitigate the oxidative damage underlying peptic ulcer pathogenesis.

6. References

1. Pham T-P-D, Vu M-L, Tran C-S, Tran LN, Tung N-T. Partially neutralized polyacrylate as a mucoadhesive polymer for gastroretentive delivery of a weakly basic drug: mechanistic study and in vivo evaluation. J Drug Deliv Sci Technol. 2026; 117(108080): 108080.
2. Goostrey T, Ross M, Soliman K, Sheardown L, Sheardown H. Mucoadhesive micelles for ophthalmic drug delivery. J Biomater Appl. 2026; 40(8): 972–86.
3. Parida N, Kokkanti RR, Biswas S, Panda A, Patnaik S, Bajoria AA. In vitro and ex vivo evaluation of a papain-loaded mucoadhesive buccal patch with potential antifibrotic and anticancer activity. Biomater Adv. 2026; 182(214731): 214731.
4. Shi Q, Meng J, Zhuang X, Ren N, Chen D, Lu F, et al. Enhancing stability and mucoadhesive properties of porous starch through chitosan surface modification for potential oral mucosal probiotic delivery. Food Hydrocoll. 2026; 174(112318): 112318.
5. Yin S, Cai Z, Chen C, Mei Y, Wei L, Liu S, et al. Comparative study on chemical constituents of medicinal and non-medicinal parts of Flos *Abelmoschus manihot*, based on metabolite profiling coupled with multivariate statistical analysis. Horticulturae. 2022; 8(4): 317.
6. Xue C, Ge H, Liu Y, Zhao Y, Huang W, Lu Z, et al. Therapeutic potential of *Abelmoschus manihot*: mechanisms of action and clinical use in traditional Chinese medicine formulas. Front Pharmacol. 2025; 16(1709530): 1709530.
7. Amelia C, Simanjuntak NJP, Novriani E. Formulation of *Abelmoschus manihot* leaf gel using carbopol and HPMC and antibacterial activity against *Pseudomonas aeruginosa*. Galen. 2025; 1(2): 181–92.
8. Zhao D, Yang S, Cai M, Bian Y, Qiu Y, Yao Q. Enzyme pretreatment combined with ultrasound-assisted aqueous biphasic extraction of flavonoids from *Abelmoschus manihot* (L.) leaves: Process optimization, antioxidant activity, and molecular docking. Food Chem. 2026; 502(147651): 147651.
9. Yin J, Chen S, Xie L, Wei L, Yu X, Yu J, et al. Efficacy and safety of *Abelmoschus manihot* in the treatment of type 2 diabetes and early diabetic kidney disease: a multicenter randomized, open-label, parallel-controlled

clinical trial. Chin Med J (Engl). 2026.

10. Lv C, Hou J, Sun H, Su W, Li Z, Wu Y, et al. Total flavones from *Abelmoschus manihot* (L.) Medik. [Malvaceae] extract ameliorates diabetic liver injury: association with ferroptosis suppression and the PI3K/AKT/Nrf2 pathway. Phytomedicine. 2026; 153(157940): 157940.
11. Varma P, Suresh R. Nanotechnology in phytopharmacology and phytomedicine: enhancing the bioavailability of curcumin (*Curcuma longa*), flavonoids, and alkaloids. J Phytopharmacology Phytomed. 2025; 2(1): 35–42.
12. Hu L, Luo Y, Yang J, Cheng C. Botanical flavonoids: Efficacy, absorption, metabolism and advanced pharmaceutical technology for improving bioavailability. Molecules. 2025; 30(5): 1184.
13. Bodakowska-Boczniewicz J, Garncarek Z. Use of naringinase to modify the sensory quality of foods and increase the bioavailability of flavonoids: a systematic review. Molecules. 2025; 30(11): 2376.
14. Ye L-S, Mu H-F, Wang B-L. Advances in flavonoid bioactivity in chronic diseases and bioavailability: transporters and enzymes. J Asian Nat Prod Res. 2025; 27(6): 805–33.
15. Zizzo MG, Terracina F, Buzzanca C, Scirè S, Dina RM, Aloi N, et al. Controlled release and enhanced bioavailability of spray-dried microparticles loaded with vitamins and natural flavonoids. 2026.
16. Janouchová V, Hurtová M, Kočová Vlčková H, Lomozová Z, Pourová J, Nováková L, et al. Glucuronidated hydroxyphenylacetic and hydroxyphenylpropanoic acids as standards for bioavailability studies with flavonoids. ACS Omega. 2026; 11(1): 1620–9.
17. Huo J, Hu S-K, Yuan R. Threshold and stability results for an age-structured SIR epidemic model with spatial diffusion. J Math Anal Appl. 2026; 556(1): 130231.
18. Wang Y-X. Effects of diffusion on a predator-prey model: Homogeneity vs heterogeneity. J Math Anal Appl. 2026; 556(1): 130233.
19. Garzó V, Brito R, Soto R. Applications of the kinetic theory for a model of a confined quasi-two dimensional granular mixture: Stability analysis and thermal diffusion segregation. Phys Fluids. 2024; 36(3).
20. Kimura K, Higuchi S. Anomalous diffusion analysis of the lifting events in the event-chain Monte Carlo for the classical XY models. Europhys Lett. 2017; 120(3): 30003.